Substrate Binding Affinity of *Pseudomonas aeruginosa* Membrane-Bound Lytic Transglycosylase B by Hydrogen−Deuterium Exchange MALDI MS†

Christopher W. Reid,‡ Dyanne Brewer,§ and Anthony J. Clarke*,‡,||

Guelph-Waterloo Center for Graduate Work in Chemistry and Biochemistry, University of Guelph, Guelph, Ontario, N1G 2W1, Canada, Biological Mass Spectrometry Facility, Department of Molecular Biology and Genetics, University of Guelph, Guelph, Ontario, N1G 2W1, Canada, and Department of Microbiology, University of Guelph, Guelph, Ontario, N1G 2W1, Canada

Received March 13, 2004; Revised Manuscript Received July 2, 2004

ABSTRACT: Lytic transglycosylases cleave the β-(1→4)-glycosidic bond in the bacterial cell wall heteropolymer, peptidoglycan, between the *N*-acetylmuramic acid (MurNAc) and *N*-acetylglucosamine (GlcNAc) residues with the concomitant formation of a 1,6-anhydromuramoyl residue. With 72% amino acid sequence identity between the enzymes, the theoretical structure of the membrane-bound lytic transglycosylase B (MltB) from *Psuedomonas aeruginosa* was modeled on the known crystal structure of *Escherichia coli* Slt35, the soluble derivative of its MltB. Of the twelve residues in Slt35 known to make contacts with peptidoglycan derivatives in Slt35, nine exist in the same position in the *P. aeruginosa* homologue, with two others only slightly displaced. To probe the binding properties of an engineered soluble form of the *P. aeruginosa* MltB, a SUPREX method involving hydrogen/deuterium exchange coupled with MALDI mass spectrometry detection was developed. Dissociation constants were calculated for a series of peptidoglycan components and compared to those obtained by difference UV absorption spectroscopy. These data indicated that GlcNAc alone does not bind to MltB with any measurable affinity but it does contribute to the binding of GlcNAc-MurNAc-dipeptide. With the MurNAc series of ligands, significant binding contributions are made through both the *N*-acetyl and C-3 lactyl moieties of the aminosugar with additional contributions to binding provided by associated peptides.

Bacteria possess an exoskeleton called peptidoglycan (or murein) which is used to withstand the strong turgor pressure exerted on their cytoplasmic membranes. This covalent structure is composed of two alternating aminosugars**,** *N*-acetylmuramic acid (MurNAc) and *N*-acetylglucosamine (GlcNAc),[1] which are joined by β-(1→4)-glycosidic linkages. The glycan strands are interconnected by short stem peptides which are attached to the lactyl moiety of muramic acid. This cross-linking generates a three-dimensional peptidoglycan sacculus of carbohydrate and amino acids that surrounds bacteria.

The generally accepted model for the biosynthesis of peptidoglycan in *Escherichia coli* invokes enzyme complexes composed of both transferases, a collection of penicillin binding proteins (PBPs), and the lytic transglycosylases (LTs) (reviewed in ref *1*). The high molecular weight PBPs catalyze the incorporation of newly synthesized peptidoglycan precursor molecule, lipid II, into the existing sacculus at sites made available by LTs (*2*, *3*). While much effort has been made to understand the function and mechanism of action of the PBPs, the LTs have attracted considerably less attention.

The LTs are a class of bacterial autolysins that function to cleave peptidoglycan at the same site as lysozymes (EC 3.2.1.17; peptidoglycan *N*-acetylmuramoyl hydrolase), specifically the β-(1→4)-glycosidic bond between the MurNAc and GlcNAc residues. However, LTs are catalytically distinct from the hydrolytic lysozymes because they cleave peptidoglycan with the concomitant formation of 1,6-anhydro-MurNAc residues (*4*) (Figure 1). These enzymes contribute to the metabolism of peptidoglycan, but their exact role has not been determined. They have been implicated as space makers for the insertion of new peptidoglycan into the cell wall during peptidoglycan remodeling and cell growth and as cell wall "zippers" during cell division (*5*, *6*). LTs have been found associated with macromolecular transport systems such as type II secretion and the type IV pilus assembly systems (reviewed in ref *7*). They may also function in the recycling of old wall material and perhaps in the formation of pores to allow transport of DNA and proteins across the cell wall (*6*, *8*).

† These studies were supported by an operating grant (MOP90587) to A.J.C. from the Canadian Institutes of Health Research.

* To whom correspondence should be addressed. Tel: (519) 824-4120 ext 54124. Fax: (519) 837-1802. E-mail: aclarke@uoguelph.ca.

‡ Guelph-Waterloo Centre for Graduate Work in Chemistry and Biochemistry.

§ Biological Mass Spectrometry Facility, Department of Molecular Biology and Genetics.

|| Department of Microbiology.

[1] Abbreviations: AnhMurNAc, 1,6-anhydro-*N*-acetylmuramic acid; GlcNAc, *N*-acetylglucosamine; GlcNAcMurNAc dipeptide, *N*-acetylglucosamine β(1,4) *N*-acetylmuramyl L-alanine L-isoglutamine; GdmCL, guanidinium chloride; LT, lytic transglycosylase; MALDI, matrix-assisted laser desorption ionization; MltB1, membrane bound lytic transglycosylase B1; Mur, muramic acid; MurNAc, *N*-acetylmuramic acid; PBP, penicillin binding protein; sMltB, soluble derivative of membrane-bound lytic transglycosylase B1; SUPREX, stability of unpurified proteins from rates of H/D exchange.

10.1021/bi049496d CCC: $27.50
Published on Web 08/14/2004

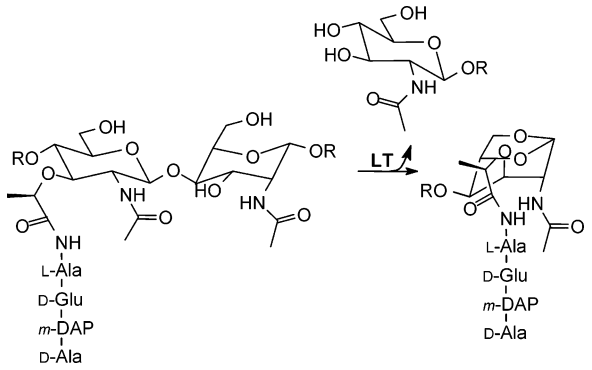

FIGURE 1: Reaction catalyzed by lytic transglycosylases (LT).

The released 1,6-anhydromuropeptides generated by LTs have been shown to cause a variety of pathobiological effects. For example, GlcNAc-AnhMurNAc-tetrapeptide released during infection with *Bordetella pertussis* has been referred to as the tracheal cytotoxin because it can directly damage HTE epithelial cells (*9*). Damage to human fallopian tubes caused by peptidoglycan-derived cytotoxin during *Neisseria gonorrhoeae* infection can also be replicated in vitro by administration of 1,6-anhydromuropeptides (*10*), and the LT responsible for its production has recently been identified (*11*). Other pathobiological effects of 1,6-anhydromuropeptides include pyrogenicity, somnogenicity, and the induction of rheumatoid arthritis (reviewed in refs *12*, *13*).

LTs appear to be ubiquitous in the eubacteria that produce peptidoglycan (viz., all but the cell wall-less mycoplasmas), and even in some lytic bacteriophages (*14*). The known and hypothetical LTs have been organized into four families based on differences within consensus signature sequences around their putative core catalytic domains (*14*). *Pseudomonas aeruginosa*, a Gram-negative, human opportunistic pathogen often associated with morbidity and mortality among cystic fibrosis patients (*15*), produces four family 3 LTs (*14*). The genes encoding all four have been cloned and expressed in *E. coli* (*16*, unpublished data). *P. aeruginosa* MltB1 shares 72% amino acid identity with the *E. coli* enzyme, and both have been demonstrated to be lipoproteins (*16*−*18*). The other three homologues are 41%, 34%, and 31% identical to the *E. coli* enzyme, but they are expressed as soluble proteins (*16*). All four family 3 enzymes from *P. aeruginosa* contain an invariant glutamyl residue homologous to the putative catalytic Glu162 of *E. coli* MltB which comprises one of the family's consensus sequences (*14*).

Monitoring rates of hydrogen/deuterium (H/D) exchange associated with peptide amides has proven to be an extremely powerful technique for the study and characterization of protein stability and dynamics (*19*−*21*). H/D exchange experiments provide several benefits over traditional spectroscopic techniques, one of which is the requirement for only small amounts of protein and sample volumes. The SUPREX (stability of unpurified proteins from rates of H/D exchange) technique is a recent development which employs MALDI mass spectrometry to monitor H/D exchanges and allows for a high-throughput quantitative assay for the analysis of protein−ligand interactions (*22*). Using the SUPREX methodology, the H/D exchange of protein samples in the absence and presence of ligands is monitored following their dilution into a series of deuterated exchange buffers containing different concentrations of guanidinium chloride (GdmCl). The destabilization of the protein structure caused by GdmCl has an effect on increasing rates of deuterium exchange which maybe countered by the presence of specific ligands. The difference in the rates of this H/D exchange comparing protein samples in the presence and absence of ligands as monitored by MALDI mass spectroscopy can thus be used to calculate binding data.

Previously, our laboratory was the first to provide a kinetic characterization of any of the LTs (*16*). Given their role in the growth and division of bacteria, we are interested in continuing our studies on the LTs which may lead to the rational design of a new class of antibacterial agents. Here, we apply both the SUPREX method and difference spectroscopy for determination of protein−ligand interactions in an engineered soluble form of *P. aeruginosa* MltB1 (sMltB). This is the first report of substrate affinity for this class of enzymes and provides evidence for the basic requirements of a substrate.

MATERIALS AND METHODS

Chemical Reagents and Enzymes. Complete EDTA-free protease inhibitor tablets, glycine, and isopropyl-α-D-thiogalactoside (IPTG) were purchased from Roche Molecular Biochemicals (Laval, PQ) while Poros affinity chromatography media was from Applied Biosystems (Valencia, CA). The BCA protein assay kit was obtained from Pierce (Rockford, IL). Superdex 75 FPLC column was supplied by Pharmacia Biotech (Baie d'Urfé, PQ), while Bio-Rad 50W−X4 cation-exchange resin was obtained from Bio-Rad Laboratories (Canada) Ltd. (Mississauga, ON). All other chemicals were supplied by either Sigma Chemical Co. (St. Louis, MO) or Fisher Scientific (Nepean, ON) and were of reagent grade or HPLC-grade where appropriate.

Peptidoglycan was isolated and purified from *Micrococcus luteus* as previously described (*23*). The isolated peptidoglycan was treated with DNase, RNase, and Pronase and reisolated by centrifugation as described by Glauner (*24*).

Isolation and Purification of sMltB. The production and purification to homogeneity of a soluble derivative of *P. aeruginosa* MltB1 (sMltB) from freshly transformed *E. coli* with pNBAC 54-1 (encoding His_6-tagged sMltB) was conducted as previously described (*16*). Briefly, sMltB was isolated from whole cell lysates of *E. coli* overexpressing *smltB* by metal affinity chromatography on a 4.6 mm × 100 mm Poros column using a Dionex BioLC. The protein was recovered from the column using a pH gradient (pH 7−4) at a flow rate of 3 mL/min. The purified protein was dialyzed against 1.5 l of 10 mM ammonium acetate, pH 6.5 containing 100 mM NaCl.

Assay for LT Activity. The specific activity of purified sMltB was measured using the assay developed by Blackburn and Clarke (*25*). Briefly, sMltB was incubated at 37 °C in the presence of 200−600 μg of purified peptidoglycan suspended in 50 mM sodium acetate buffer, pH 5.8 containing 0.1% Triton X-100. At appropriate intervals of time, samples were flash frozen at −78 °C to halt the reaction. The insoluble peptidoglycan was removed from the thawed samples by centrifugation (13000*g*, 15 min, 4 °C), and the recovered supernatants containing the released and soluble muropeptides were evaporated to dryness. The dried samples were hydrolyzed with 5.8 M HCl for 2 h at 98 °C and then

evaporated to dryness. The muramic acid content of the hydrolyzed samples was measured using a Beckman System Gold amino acid analyzer (Beckman Coulter Canada Inc., Mississauga, ON) with ninhydrin detection.

Analysis of Oligomerization of sMltB. The oligomerization of sMltB was assessed by size-exclusion chromatography on a Superdex 75 column using 10 mM sodium phosphate buffer, pH 7.0 as eluant at a flow rate of 0.7 mL/min. The column was standardized using a set of protein standards, BSA (66 kDa), PoaD (42 kDa) (*26*), carbonic anhydrase (29 kDa), and lysozyme (14.4 kDa).

Difference UV Absorbance Spectroscopy. Absorbance spectra of purified sMltB (7.03 FM) in 10 mM ammonium acetate buffer, pH 6.5 containing 100 mM NaCl were collected using a Beckman DU-530 spectrophotometer. Quantitative binding experiments were performed by collecting scans of sMltB after the sequential addition of ligand and incubation for 90 s at room temperature. Each scan was corrected for dilution by multiplying with a correction factor $[(\sum V_t + V_i)/V_i$, where V_t is the titration volume and V_i is the initial volume]. Scans were normalized by subtraction of the scan at zero ligand concentration (*27*). The trough to peak heights at $A_{287\,nm} - A_{281\,nm}$ or $A_{253\,nm} - A_{276\,nm}$ were plotted versus the total ligand concentration, and dissociation constants were derived using a nonlinear regression analysis with a two-site binding model (Microcal Origin 5.0).

Hydrogen−Deuterium (H/D) Exchange Experiments. The protocols used to generate the H/D denaturation curves are based on the work previously described by Powell and coworkers (*22*). Hydrogen−deuterium exchange reactions were initiated by combining 1 μL aliquots of sMltB in 10 mM ammonium acetate buffer, pH 6.5 containing 100 mM NaCl (enzyme buffer) with 9 μL volumes of the same buffer prepared in D_2O (pD 6.1, exchange buffer) containing varying concentrations of GdmCl that varied from 0 to 8 M. For protein−ligand interaction studies, 1 μL of the protein solution was combined with 1 μL of ligand in the enzyme buffer and 9 μL of exchange buffer. Samples were incubated for times ranging from 0 to 1 h at room temperature. After a specified exchange time, the protein was extracted with either a C_4 or C_{18} Zip-tip, washed with 1 to 3 volumes of ice cold 5% MeOH, and eluted into varying volumes (1−5 μL) of ice cold sinapinic acid in 65% acetonitrile with 0.1% TFA. The quenched samples (1 μL) were spotted onto the MALDI sample plate, or the internal calibration standard BSA was added prior to spotting.

Samples were analyzed on a Bruker Reflex III MALDI-TOF in reflectron mode using a 337 nm nitrogen laser set to 109−121 μJ output. One hundred to two hundred replicate MALDI mass spectra were collected, processed, and analyzed to determine an average change in mass relative to the fully protonated sample (ΔMass) at each GdmCl concentration. The mass of deuterated sMltB was determined with a two-point internal calibration utilizing BSA [M + H] and [M + 2H] as an internal standard. All H/D exchange experiments were performed in duplicate using separate preparations of enzyme. The masses of individual protein species were obtained by taking the centroid at 80% peak height.

Analysis of H/D Exchange Data. The data were plotted as ΔMass (deuterated mass − fully protonated mass) vs GdmCl concentration. A nonlinear least-squares analysis routine was used for curve fitting (Microcal Origin 5.0), and the transition midpoint of the graph was determined. The free energy of folding (ΔG_f°) for sMltB in the presence and absence of ligand was determined using eq 1:

$$-\Delta G_f^\circ = mC^{1/2}{}_{SUPREX} + RT \ln \frac{\left(\frac{\langle k_{int}\rangle t - 1}{0.693}\right)}{\frac{n^n}{2^{n-1}}[P]^{n-1}} \quad (1)$$

where m is defined as $\delta\Delta G_f^\circ/\delta$[GdmCl] (0.026 kcal mol^{-1} M^{-1} per amino acid) (*28*), $C^{1/2}{}_{SUPREX}$ is the [GdmCl] at the SUPREX transition midpoint, R is the gas constant, T is the temperature in kelvins, $\langle k_{int}\rangle$ (10^{pH-5}) is the average intrinsic exchange rate of an amide proton (*22*), t is the H/D exchange time, n is the number of subunits in the protein, and [P] is the protein concentration expressed in n-mer equivalents. The experimental m value for ligand binding was determined by incubating sMltB for varying exchange times in the presence of MurNAc. Plotting of $\Delta\Delta G_f$ as a function of $C^{1/2}{}_{SUPREX}$ gave a slope corresponding to m_b. The corrected m value was then calculated using the equation $m = m_p + m_b$, where m_p was equivalent to the m value associated with the protein's folding/unfolding reaction and was estimated from the data in Myers et al. (*28*), and the m_b component was the m value associated with the binding reaction.

Dissociation constants (K_d) were calculated from $\Delta\Delta G_f^\circ$ values using eq 2:

$$\Delta\Delta G_f^\circ = -nRT \ln[1 + ([L]/K_d)] \quad (2)$$

where $\Delta\Delta G_f^\circ$ is the difference between ΔG_f° (ligand bound) and ΔG_f° in the absence of ligand, n is the number of binding sites, and [L] is the ligand concentration. All binding experiments were performed using a 50−100-fold excess of ligand. The number of binding sites (n) was determined by measuring ligand-induced stability changes at varying concentrations of ligand. Thus, samples of protein were incubated with 1, 2, 4, 50, and 100 equiv of MurNAc-dipeptide for 15 min at ambient temperature prior to performing the H/D exchange reactions. Values of both $\Delta\Delta G_f$ and $C^{1/2}{}_{SUPREX}$ were calculated and compared.

Other Analytical Methods. Sodium dodecyl sulfate (SDS)−polyacrylamide gels were prepared using the discontinuous buffer system of Laemmli (*29*) and sample buffer containing SDS and 2-mercaptoethanol. Gels were stained with Coomassie Brilliant Blue R-250 as described by Bollag et al. (*30*). Protein concentrations were measured using the Pierce BCA protein assay kit with BSA serving as the standard.

For protein modeling, the amino acid sequence of sMltB (P41052) lacking the 17 N-terminal amino acids corresponding to the signal sequence and the lipidated cysteine residue was modeled using 3D-PSSM (*31*, *32*) and the high-resolution three-dimensional structure of *E. coli* Slt35 (1QDR) as the template.

RESULTS

Hypothetical Structure of sMltB. The *P. aeruginosa* sMltB sequence shares 72% identity with *E. coli* Slt35, the naturally derived 36 kDa soluble derivative of MltB. Given this strong sequence similarity, the hypothetical three-dimensional struc-

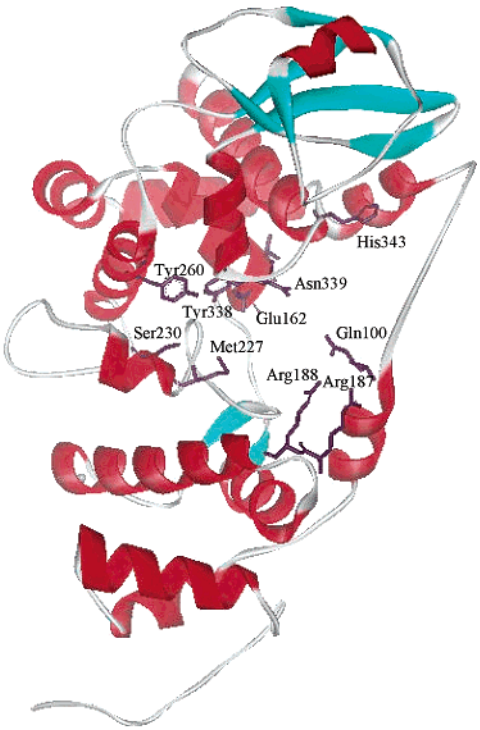

FIGURE 2: Hypothetical structure of *P. aeruginosa* sMltB modeled on the crystal structure of *E. coli* Slt35 (1QDR). The positions of the residues identified in Table 1 are shown.

Table 1: Comparison of Residues in the Peptidoglyan-Binding Cleft Slt35 and sMltB

subsite	Slt35−murodipeptide complex contacts[a]	sMltB equivalent residue[b]
−2	Tyr259 Oη···O3 GlcNAc	Tyr260
	Ser230 Oγ···O7 GlcNAc	**Ser230**
	Met227 N···O7 GlcNAc	**Met227**
−1	Gln98 Nϵ2···O7 MurNAc	Gln100
	Tyr338 Oη···O6 MurNAc	**Tyr338**
	Glu162 Oϵ2···O6 MurNAc	**Glu162**
	Arg187 Nη—CO D-Glu	**Arg187**
	Arg188 Nη···O10 MurNAc	**Arg188**
+1	Glu162 Oϵ2···O3 GlcNAc	**Glu162**
	Asn339 Nδ2···O4 GlcNAc	**Asn339**
+2	Val161 O···O6 MurNAc	**Val161**
	Gln207 Oϵ1···O1 MurNAc	Gly207
	His343 Nϵ···Oδ D-Glu	**His343**

[a] Residues within 3.5 Å of muropeptides observed in crystal structure of Slt35-muropeptide complex and proposed to form (···) hydrogen bonds or (—) salt bridge (*34*). [b] Residues in bold denote equivalence in both identity and sequence position.

ture of sMltB was modeled on the high-resolution crystal structure of Slt35 (*33*, *34*). The *E*-value associated with this prediction was 8.22×10^{-40} indicating a very high level of confidence (*E*-values below 0.05 are highly confident) (*31*, *32*). Not surprisingly then, the model predicted a structure for sMltB (Figure 2) that was nearly superimposable on that of Slt35. Thus, like the Slt35, sMltB is composesd of three domains, α, β, and core, where the core domain resembles the fold of the goose-type lysozymes. This similarity with Slt35 extended to the size of the active-site cleft accommodating a tetrasaccharide ligand (i.e., four sub-sites) and the positioning of active-site residues known to make contacts with bound ligands (Table 1). Thus, Glu162, the putative catalytic residue, is found within a deep groove of the core

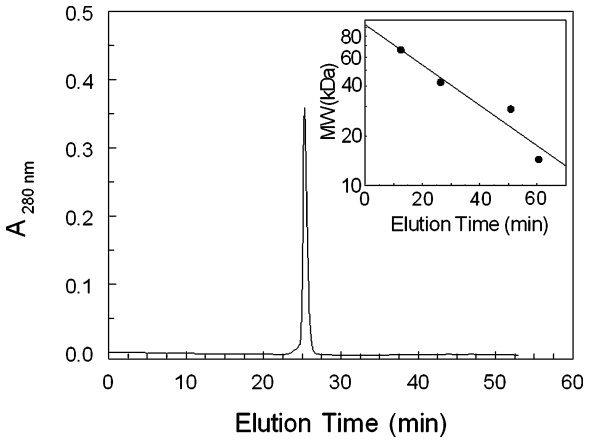

FIGURE 3: Size-exclusion chromatography of sMltB on Superdex 75 with 10 mM sodium phosphate buffer, pH 7.0 as eluant. Inset: Calibration curve for the column.

domain which also contains 11 of the 12 residues known to form either hydrogen bonds or salt bridges to peptidoglycan fragments (*33*). Nine of these identical 11 residues are located in the same positions as their Slt35 counterparts. Residues 101−108 form the "exo-loop" seen in the Slt35 structure (residues 99−108) which is thought to impose the exo-lytic activity of these enzymes (viz., release of disaccharide peptides from the nonreducing ends of peptidoglycan strands) (*34*). Finally, the predicted catalytic domain also possesses the EF-hand loop, involving residues 237−245 (seven of the nine residues are identical while the other two represent conservative replacements) which is observed in the Slt35 structure (residues 237−245) (*34*) and known to bind calcium (*35*).

Oligomerization of sMltB. The quaternary structure of a protein has to be established to properly calculate the dissociation constants for protein−ligand interactions using the SUPREX method. The ability of sMltB to form multimers was examined by size-exclusion chromatography on Superdex 75. As seen in Figure 3, sMltB eluted as a single symmetrical peak with an apparent molecular mass of 46.2 kDa. This corresponds closely to the theoretical mass of the protein (38973 Da) and that determined by SDS−PAGE (40.5 kDa) (data not shown), thus indicating that sMltB remains in monomeric form.

H/D Exchange Conditions. The denaturation profile of sMltB was investigated by incubating the protein in GdmCl for exchange times varying from 5 to 60 min. The mass spectra of sMltB in the presence of exchange buffer showed an increase in the protein mass with increasing denaturant concentration (Figure 4). An incubation time of 15 min at room temperature resulted in a sigmoidal curve and appeared to be optimal for this protein (data not shown).

Extraction of the protein from the exchange buffer was effected by the use of C_4 or C_{18} Zip-tips. Effective and reproducible concentration and washing of the protein was obtained with the C_4 Zip-tip. The protein was eluted into varying volumes of sinapinic acid matrix (1−5 μL) with and without the internal calibration standard BSA present. Extraction of sMltB into 5 μL of sinapinic acid was found to sufficiently elute the protein. MALDI MS analysis of sMltB showed that the addition of BSA enhanced the ionization of sMltB and thus provided an increase in sensitivity.

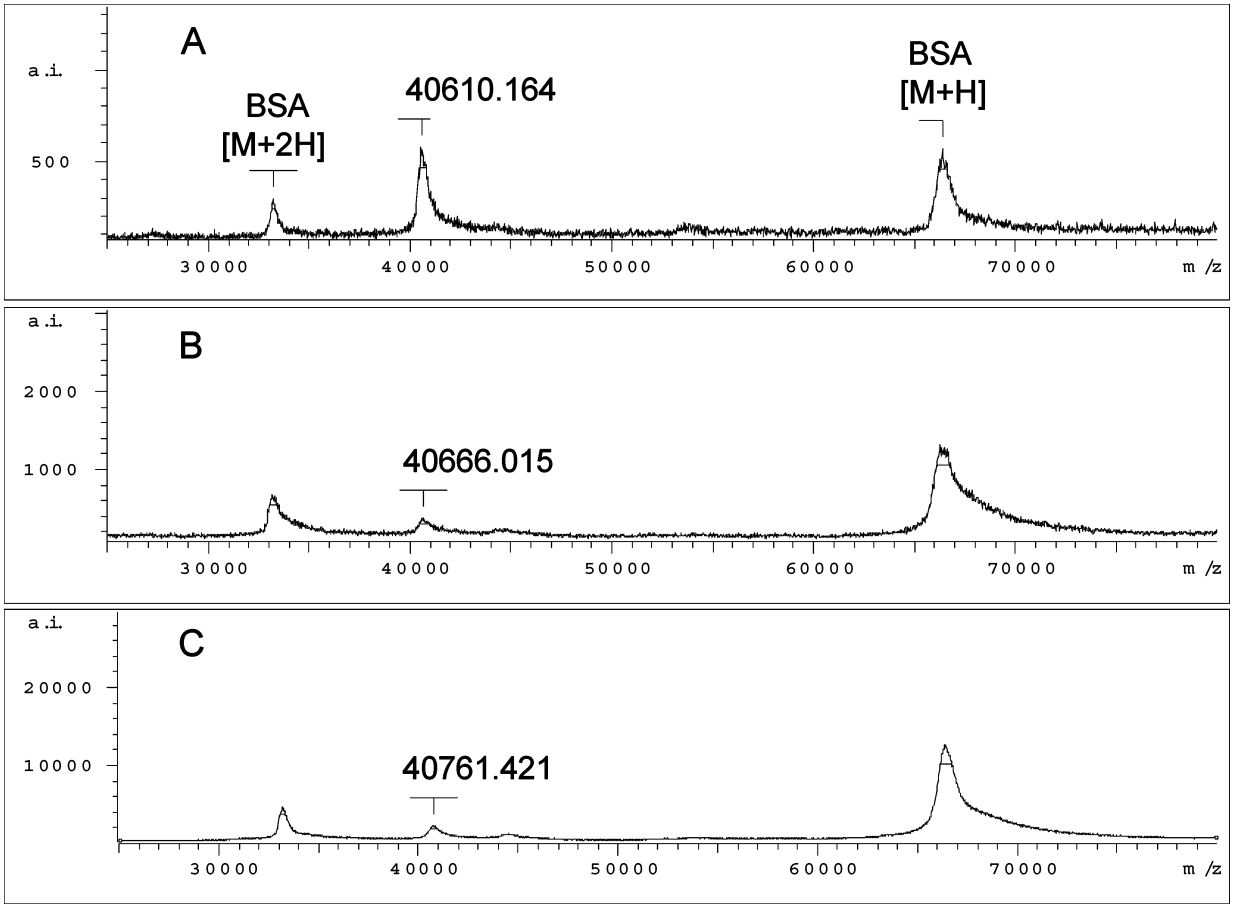

FIGURE 4: Representative MALDI MS spectra of sMltB. The spectra were obtained after incubation of sMltB in the absence of ligand for 15 min in H/D exchange buffer containing (A) 0 M, (B) 1 M, and (C) 3 M GdmCl.

Analysis of MALDI MS peak widths of sMltB under the exchange conditions using the method described by Robertson and co-workers (*36*, *37*) indicated that the protein followed EX2 exchange. With the EX2 exchange limit, only one population of deuterated sMltB molecules is detected by MALDI MS during the time course of H/D exchange resulting in relatively symmetrical peaks. Also, analysis of protein refolding of sMltB by both mass spectrometry (*38*) and gel filtration (*39*) did not result in the detection of intermediates (data not shown) indicating that the enzyme appears to follow a two-state folding process.

Denaturant Dependence of Binding Reaction and Determination of Binding Site Number. The dependence of denaturant on the binding reaction of various ligands to sMltB was determined by measuring ligand-induced stability changes at different $C^{1/2}_{\mathrm{SUPREX}}$ values (Figure 5). The stability changes observed with *N*-acetylmuramic acid at different exchange times revealed that the $\Delta\Delta G_f^\circ$ values are linearly dependent on the $C^{1/2}_{\mathrm{SUPREX}}$ values used to calculate the ΔG_f° value for the complex (Figure 5). From this linear relationship the m_b value ($\delta\Delta G_f^\circ/\delta$[GdmCl]) of -9.10 kcal mol^{-1} M^{-1} was obtained.

To determine the number of binding sites, sMltB was incubated with varying concentrations of MurNAc-dipeptide and the apparent SUPREX-derived $\Delta\Delta G_f^\circ$ values were calculated. The $\Delta\Delta G_f^\circ$ values obtained from these ligand dependent data were then used in eq 2 to calculate the K_d values. Using an *n*-value of 2 (corresponding to 2 MurNAc-dipeptide binding sites) provided the best fit of the observed data. The determination of two binding sites in sMltB for this ligand is in agreement with that observed directly by X-ray crystallography for the Slt35 homologue (*33*, *34*).

K_d Determinations. Using the SUPREX procedure, K_d values were calculated on the basis of sMltB existing in a monomeric state, as previously determined by size-exclusion chromatography and assuming binding of two ligands (i.e., $n = 2$). A shift in the denaturation profile of sMltB by H/D exchange was observed when Mur and its adducts, MurNAc, MurNAc-dipeptide, and GlcNAcMurNAc-dipeptide, were added to reaction mixtures. Titration of the enzyme with these peptidoglycan derivatives thus permitted the determination of K_d values from which $\Delta G_{\mathrm{binding}}$ values were calculated. The results of these binding experiments are summarized in Table 2. From these data, it is clear that the presence of each additional moiety enhanced binding of Mur to sMltB with the greatest gain in affinity being conferred by the acetylation of its amine followed by the addition of GlcNAc to the MurNAc-dipeptide. The free energy contributions for the various substitutions associated with the peptidoglycan ligands are summarized in Figure 6. In contrast to the effect observed with these Mur-containing ligands, no shift was observed in the denaturation profile of sMltB when GlcNAc alone was added to the H/D exchange buffer.

The binding data obtained by the SUPREX method were in close agreement with the K_d values obtained by difference UV absorbance spectroscopy. Difference spectra showed a negative trough at 277 nm with a red shift upon binding of MurNAc-containing ligands to the protein. These red shifts

Table 2: Binding Affinity of Ligands to *P. aeruginosa* sMltB

	SUPREX				UV difference	
ligand	$C^{1/2}_{SUPREX}$[a] (M)	$\Delta\Delta G_f$[b] (kJ/mol)	K_d (mM)	$\Delta G_{binding}$[c] (kJ/mol)	K_d[d] (mM)	$\Delta G_{binding}$[c] (kJ/mol)
	1.75 ± 0.012[e]					
GlcNAc	nd[f]	nd	nd		nd	
Mur	2.22 ± 0.036	-0.460 ± 0.059	3.78 ± 0.502	-13.7		
MurNAc	2.87 ± 0.604	-1.02 ± 0.214	1.30 ± 0.283	-16.4	1.67 ± 0.156	-15.7
MurNAc-dipeptide	3.40 ± 0.495	-1.54 ± 0.224	1.05 ± 0.356	-16.9	0.309 ± 0.160	-19.1
GlcNAC-MurNAc-dipeptide	3.67 ± 0.106	-1.79 ± 0.383	0.467 ± 0.051	-18.9	0.175 ± 0.079	-20.6

[a] All SUPREX experiments were performed at room temperature with an exchange time of 15 min with GdmCl as denaturant. [b] Values calculated using ΔG_f values obtained from eq 1 (i.e., $\Delta G_{f(ligand)} - \Delta G_{f(no\ ligand)}$). [c] Values calculated from the averaged experimentally obtained K_d values. [d] Standard deviation of 3 separate experiments. [e] Standard deviation of 2 separate experiments using different preparations of sMltB. [f] Not detected.

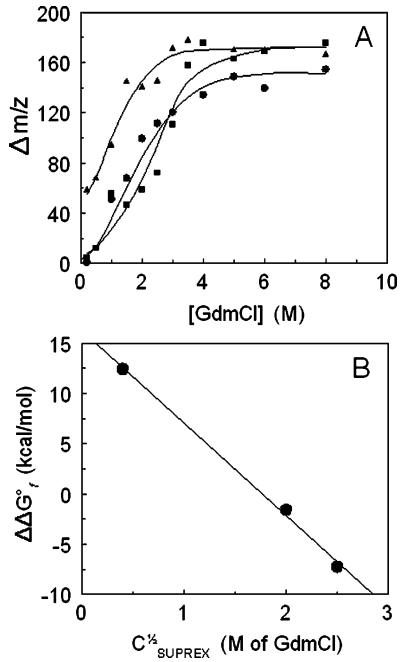

FIGURE 5: Representative SUPREX curves for sMltB in the presence of MurNAc. (A) Denaturation curves of 5.7 μM sMltB in the presence of 295 μM MurNAc and H/D exchange buffer containing the indicated concentrations of GdmCl following incubation at ambient temperature for (●) 5 min, (■) 15 min, and (▲) 30 min. These curves yielded $C^{1/2}_{SUPREX}$ values of 0.1, 3.25, and 3.75 M GdmCl, respectively. (B) Determination of binding SUPREX m_b value.

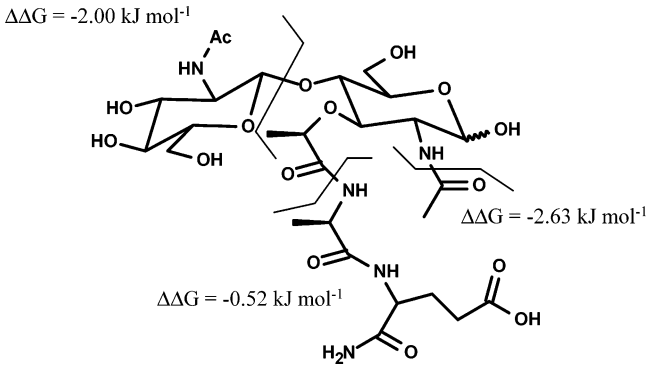

FIGURE 6: Free energy contribution of structural features of peptidoglycan subunit GlcNAc-MurNAc-dipeptide to binding to sMltB. The $\Delta\Delta G$ values were calculated using ΔG values listed in Table 2 and are relative to the next smallest peptidoglycan substrate (e.g., $\Delta G_{MurNAc} - \Delta G_{Mur}$).

indicate a conformational change of an aromatic residue to a more nonpolar environment. Saturation curves of sMltB titrated with these ligands and transformation of the data provided the K_d values listed in Table 2. Again, in contrast, addition of GlcNAc alone to sMltB showed a small positive peak at 277 nm which can be attributed to nonspecific binding to the protein.

DISCUSSION

Our use of H/D exchange coupled with MALDI mass spectrometry has proven to be a highly effective tool for studying the substrate affinity of carbohydrate-binding proteins. The dissociation constants (K_d values) determined by the method sMltB-complexes with small ligands were generally in good agreement with K_d values measured by the more conventional difference UV spectroscopy method. The slight variance between these ligand binding data is consistent with that found by Powell et al. in their study of four different model protein ligand complexes (*22*). The main advantage that the SUPREX technique holds over other more traditional techniques is that only small amounts of protein and ligand are required for the experiments. This is especially advantageous when attempting to study membrane-bound or -associated enzymes that are sparingly soluble, as is the case with the LTs. It is also conceivable that future studies could involve the membrane-bound form of the enzyme provided that an appropriate matrix is used to permit its laser desorption ionization for MS analysis. That the SUPREX technique lends itself to a high-throughput assay for the assessment of changes in substrate binding is an added bonus.

Analysis of the binding affinity of the substrates presented in Table 2 identifies the important structural features involved in ligand binding to sMltB (Figure 6). As observed with both the SUPREX and difference spectroscopic techniques, GlcNAc alone does not appear to bind with any measurable affinity to sMltB while K_d values of 3.8 mM and 1.3 mM were determined for Mur and MurNAc, respectively. The lack of detectable GlcNAc binding was not totally unexpected given previous observations that this monosaccharide does not inhibit sMltB activity (*16*). In addition, kinetic studies with both sMltB (*16*) and the *E. coli* homologue (*40*) have shown the absolute requirement of peptide side chains on peptidoglycan for lytic activity by these enzymes. Unlike muramidases such as hen egg-white lysozyme, the LTs are incapable of cleaving chitin (poly GlcNAc) or any of its soluble and chromogenic/fluorgenic derivatives, such as nitrophenyl- or methylumbelliferyl-chitooligosaccharides. In this regard, however, it has been proposed that the LTs may require elements of MurNAc residues and/or associated

peptides for their mechanism of action in a substrate-assisted manner (*33*).

The only difference between the structures of GlcNAc and MurNAc is the presence of a D-lactyl group at C-3 of the latter (Figure 1), and, as indicated in Figure 6, major contributions to binding of the peptidoglcyan-derived ligands occur through this moiety and its associated peptides. Thus, the presence of the C-3 lactyl moiety of muramyl residues appears to be vital for the proper orientation of ligands into the active site cleft of sMltB, and presumably all other LTs. This is reflected by the extensive network of contacts that are observed in the crystal structure of *E. coli* Slt35−ligand complexes between the enzyme and both the D-lactyl moiety and the stem peptide of the ligands at subsites −1 and +2 (*33*) (Table 1). For subsite −1 which is adjacent to the site of cleavage these include a hydrogen bond between the invariant Arg188 residue and the carbonyl of the D-lactyl group, and a salt bridge between the highly conserved Arg187 residue (*14*) and the free α-carboxyl group of the γ-glutamyl residue of the stem peptide. Likewise at subsite +2, contacts include a hydrogen bond between the analogous carboxyl group of the stem peptide on this second MurNAc-dipeptide and His343. It would seem safe to assume that similar binding interactions would exist in the *P. aeruginosa* sMltB−substrate complex given that (i) the enzyme shares 72% sequence identity with Slt35 (*14*), (ii) all but three of the twelve residues known to form hydrogen bonds to ligand exist in exactly the same positions in the sMltB sequence (Table 1; two of the three are identical but simply shifted by one or two residues), (iii) the two enzymes share identical secondary structure composition as determined experimentally (*41*, *42*), and (iv) the sMltB sequence could be modeled onto the three-dimensional structure of Slt35 with very high confidence. It should also be noted that the family 1 *E. coli* Slt70 catalytic domain is very similar to that of family 3 *E. coli* Slt35 (root-mean-square deviation of 1.7 Å for 100 Cα atoms) despite lacking any significant overall sequence similarity (*33*, *34*). Preliminary support for the participation of sMltB residues in ligand binding is provided by observations that the Arg188Ala mutant and Arg187Ala/Arg188Ala double mutant derivatives of the enzyme have diminished specific activity (70% and 32% of wild-type, respectively) (*41*). While GlcNAc alone does not appear to bind to sMltB, its presence to extend the glycan chain does enhance binding affinity of MurNAc ligands as reflected in the ΔΔG of 2 kJ/mol calculated from the K_d values obtained for MurNAc-dipeptide and GlcNAcMurNAc-dipeptide. This enhancement in binding was expected given, as noted above, that the active site of MltB is composed of four subsites and a number of contacts are observed in the crystal structure of *E. coli* Slt35−ligand complexes at subsites −2 and +1 which accommodate GlcNAc residues (Table 1).

Although disassociation constants obtained for small soluble substrates in vitro are useful in assessing the requirements for substrate binding, the situation and conditions of the experimentation do not accurately reflect very well what is occurring in vivo/situ. Hence, the relatively weak interactions of sMltB with the various ligands presented in this study needs to be viewed in the context of those interactions involving other enzymes that act on insoluble substrates. For example, the apparent association constants obtained for the binding of soluble cellulose fragments to a variety of cellulases are weak and in the mM range (*27*, *43*). Taken in context, these enzymes are naturally in the presence of insoluble substrate (cellulose, peptidoglycan) and act at the solution/solid interface. In its natural state, MltB1 is lipid anchored to the outer membrane and likely comprises a biosynthetic complex with the PBPs that are associated with the cytoplasmic (inner) membrane (*3*). This complex is thus thought to sandwich the insoluble peptidoglycan and be forced into place by the internal turgor pressure of the cell. Clearly, the in vitro conditions of our experiments do not come close to mimicking this natural situation. Finally, it should be noted that the K_d values obtained with the more extensive peptidoglycan fragments used in this study do approach the apparent K_M value of 72.1 μM estimated for sMltB acting on the insoluble substrate (*16*).

By virtue of its unique chemical structure in nature and its importance to bacterial cell viability, the metabolism of peptidoglycan has been well exploited as a target for antibacterial drug development. Unfortunately, some of these antibacterials are quickly becoming irrelevant for clinical use as drug resistance levels increase in human and animal pathogens. For example, the prevalence of β-lactamases among a variety of important pathogens has seriously compromised the general therapeutic use of the β-lactams (monobactams, penicillins, cephalosporins), compounds that are functional analogues of the stem peptide portion of the peptidoglycan-repeating unit. Using a different mode of resistance, vancomycin-resistance in enterococci (VRE) arises when alterations to the stem peptide of the organism are made resulting in a decreased affinity for the antibiotic (*44*). In contrast to the chemically heterogeneous stem peptide, all peptidoglycans characterized to date are composed of the same repeat unit of disaccharide (viz., GlcNAc-β(1→4)-MurNAc). This consistency underscores the prospect of designing antibacterials that target enzymes involved in its metabolism for which the development of resistance would be more difficult to achieve. Thus, despite the alarming trends of antibiotic resistance, the metabolism of peptidoglycan still presents potential targets for new drug development, including the LTs. The apparent ubiquity of LTs among the bacteria (*14*) further supports their potential as an antibacterial target, and the application of the SUPREX method described herein will greatly facilitate their further development.

REFERENCES

1. Young, K. D. (2003) Bacterial Shape, *Mol. Microbiol. 45*, 571−580.
2. Ghysen, J.-M., and Hakenbeck, R. (1994) *Bacterial cell wall*, pp 131−166, Elsevier, Amsterdam, The Netherlands.
3. Höltje, J.-V. (1998) Growth of the stress-bearing and shape-determining murein sacculus of *Escherichia coli*, *Microbiol. Mol. Biol. Rev. 62*, 181−203.
4. Höltje, J.-V., Mirelmen, D., Sharon, N., and Schwarz, U. (1975) Novel type of murein transglycosylase in *Escherichia coli*, *J. Bacteriol. 124*, 1067−1076.
5. Höltje, J.-V., and Tuomanen, E. I. (1991) The murein hydrolases of *Escherichia coli*: properties, functions and impact on the course of infections *in vivo*, *J. Gen. Microbiol. 137*, 441−454.
6. Goodell, E. W. (1985) Recycling of murein by *Escherichia coli*, *J. Bacteriol. 163*, 305−310.
7. Koraimann, G. (2003) Lytic transglycosylases in macromolecular transport systems of Gram-negative bacteria, *Cell. Mol. Life Sci. 60*, 2371−2388.

8. Dijkstra, A. J., and Keck, W. (1996) Peptidoglycan as a barrier to transenvelope transport, *J. Bacteriol. 178*, 5555−5562.
9. Luker, K. E., Collier, J. L. Kolodziej, E. W., Marshall, G. R., and Goldman, W. E. (1993) *Bordetella pertussis* tracheal cytotoxin and other muramyl peptides: distinct structure−activity relationships for respiratory epithelial cytopathology, *Proc. Natl. Acad. Sci. U.S.A. 90*, 2365−2369.
10. Melly, M. A., McGee, Z. A., and Rosenthal, R. S. (1984) Ability of monomeric peptidoglycan from *Neisseria gonorrhoeae* to damage human fallopian-tube mucosa, *J. Infect. Dis. 149*, 378−386.
11. Cloud, K. A., and Dillard, J. P. (2002) A lytic transglycosylase of *Neisseria gonorrhoeae* is involved in peptidoglycan-derived cytotoxin production, *Infect. Immun. 70*, 2752−2757.
12. Clarke, A. J., and Dupont, C. (1992) *O*-Acetylated peptidoglycan: its occurrence, pathobiological significance and biosynthesis, *Can. J. Microbiol. 38*, 85−91.
13. Clarke, A. J., Strating, H., and Blackburn, N. T. (2000) Pathways for the *O*-acetylation of bacterial cell wall polysaccharides, in *Glycomicrobiology* (Doyle, R. J., Ed.), pp 187−223, Plenum Publishing Co. Ltd., New York.
14. Blackburn, N. T., and Clarke, A. J. (2001) Identification of four families of microbial lytic transglycosylases, *J. Mol. Evol. 52*, 78−84.
15. Govan, J. R. W., and Deretic, V. (1996) Microbial pathogenesis in cystic fibrosis: mucoid *Pseudomonas aeruginosa* and *Burkholderia cepacia*, *Microbial Rev. 60*, 539−574.
16. Blackburn, N. T., and Clarke, A. J. (2002) Characterization of soluble and membrane-bound family 3 lytic transglycosylases from *Pseudomonas aeruginosa*, *Biochemistry 41*, 1001−1013.
17. Engel, H., Smink, A. J., van Wijngaarden, L., and Keck, W. (1992) Murein-metabolizing enzymes from *Escherichia coli*: existence of a second lytic transglycosylase, *J. Bacteriol. 174*, 6394−6403.
18. Ehlert, K., Höltje, J-.V., and Templin, M. F. (1995) Cloning and expression of a murein hydrolase lipoprotein from *Escherichia coli*, *Mol. Microbiol. 16*, 761−768.
19. Ghaemmaghami, S., Fitzgerald, M..C., and Oas, T. G. (2000) A quantitative, high-throughput screen for protein stability, *Proc. Natl. Acad. Sci. U.S.A. 97*, 8296−8301.
20. Powell, K. D., and Fitzgerald, M. C. (2001) Measurements of protein stability by H/D exchange and matrix-assisted laser desorption/ionization mass spectrometry using picomoles of material, *Anal. Chem. 73*, 3300−3304.
21. Yan, X., Broderick, D., Leid, M. E., Schimerlik, M. I., and Deinzer, M. L. (2004) Dynamics and ligand-induced solvent accessibility changes in human retinoid x receptor homodimer determined by hydrogen deuterium exchange and mass spectrometry, *Biochemistry 43*, 909−917.
22. Powell, K. D., Ghaemmaghami, S., Wang, M. Z., Ma, L., Oas, T. G., and Fitzgerald, M. C. (2002) A general mass spectrometry-based assay for the quantitation of protein−ligand binding interactions in solution, *J. Am. Chem. Soc. 124*, 10256−10257.
23. Clarke, A. J. (1993) Compositional analysis of peptidoglycan by high-performance anion-exchange chromatography. *Anal. Biochem. 212*, 344−350.
24. Glauner, B. (1988) Separation and quantification of muropeptides with high-performance liquid chromatography, *Anal. Biochem. 172*, 451−464.
25. Blackburn, N. T., and Clarke, A. J. (2000) Assay for lytic transglycosylases: a family of peptidoglycan lyases, *Anal. Biochem. 284*, 388−393.
26. Weadge, J. T., and Clarke, A. J. (2003) Kinetic analysis of a peptidoglycan de-*O*-acetylase from *Neisseria gonorrhoeae*, Abstract *101st ASM General meeting.*
27. Boraston, A. B., Chiu, P., Warren, R. A. J., and Kilburn, D. G. (2000) Specificity and affinity of substrate binding by a family 17 carbohydrate-binding module from Clostridium cellulovorans cellulase 5A, *Biochemistry 39*, 11129−11136.
28. Myers, J. K., Pace, C. N., and Scholtz, J. M. (1995) Trifluoroethanol effects on helix propensity and electrostatic interactions in the helical peptide from ribonuclease T1, *Protein Sci. 4*, 2138−2148.
29. Laemmli, U. K. (1970) Cleavage of structural proteins during the assembly of bacteriophages T4, *Nature 227*, 680−685.
30. Bollag, M., Rozycki, M. D., and Edelstein, S. J. (1996) *Protein Methods*, 2nd ed., pp 107−154, Wiley-Liss, Toronto.
31. Kelly, L. A., MacCallum, R. M., and Sternberg, M. J. E. (2000) Enhanced genome annotation using structural profiles in the program 3D-PSSM, *J. Mol. Biol. 299*, 499−520.
32. Bower, M., Cohen, F. E., and Dunbrack, R. L., Jr. (1997) Prediction of protein side-chain rotamers from a backbone-dependent rotamer library: a new homology modeling tool, *J. Mol. Biol. 267*, 1268−1282.
33. van Asselt, Kalk, K. H., and Dijkstra, B. W. (2000) Crystallographic studies of the interaction of *Escherichia coli* lytic transglycosylase Slt35 with peptidoglycan, *Biochemistry 39*, 1924−1934.
34. van Asselt, E. J., Dijkstra, A. J., Kalk, K. H., Takacs, B., Keck, W., and Dijkstra, B. W. (1999) Crystal structure of *Escherichia coli* lytic transglycosylase Slt35 reveals a lysozyme-like catalytic domain with an EF-hand, *Structure 7*, 1167−1180.
35. van Asselt, E. J., and Dijkstra, B. W. (1999) Binding of calcium in the EF-hand of *Escherichia coli* lytic transglycosylase Slt35 is important for stability, *FEBS Lett. 458*, 429−435.
36. Arrington, C. B., and Roberston, A. D. (2000) Correlated motions in native proteins from MS analysis of NH exchange: evidence for a manifold of unfolding reactions in ovomucoid third domain, *J. Mol. Biol. 300*, 221−232.
37. Ferraro, D. M., and Robertson, A. D. (2004) EX1 Hydrogen exchange and protein folding, *Biochemistry 43*, 587−594.
38. Pan, H., Raza, A. S., and Smith, D. L. (2004) Equilibrium and kinetic folding of rabbit muscle triosephoshate isomerase by hydrogen exchange mass spectrometry, *J. Mol. Biol. 336*, 1251−1263.
39. Srimathi, T., Kumar, T. K. S., Kathir, K. M., Chi, Y.-H., Srisailam, S., Lin, W.-Y., and Chiu, Y. (2003) Structurally homologus all beta-barrel proteins adopt different mechanisms of folding, *Biophys. J. 85*, 459−472.
40. Romeis, T., Vollmer, W., and Höltje, J.-V. (1993) Characterization of three different lytic transglycosylases from *Escherichia coli*, *FEMS Microbiol. Lett. 111*, 141−146.
41. Blackburn, N. T. (2001) Characterization of family three lytic transglycosylases from *Pseudomonas aeruginosa*, Ph.D. Thesis, University of Guelph.
42. Reid, C. W., Blackburn, N. T., Legarree, B. A., Auzanneau, F.-I., and Clarke, A. J. (2004) Inhibition of membrane-bound lytic transglycosylase B by NAG-thiazoline, *FEBS Lett.* (submitted).
43. Dam, T. K., Roy, R., Page, D., and Brewer, C. F. (2002) Thermodynamic binding parameters of individual epitopes of multivalent carbohydrates to concanavalin a as determined by "reverse" isothermal titration microcalorimetry, *Biochemistry 41*, 1359−1363.
44. Bugg, T. D., Wright, G. D., Dutka-Malen, S., Arthur, M., Courvalin, P., Walsh, C. T. (1991) Molecular basis for vancomycin resistance in *Enterococcus faecium* BM4147: biosynthesis of a depsipeptide peptidoglycan precursor by vancomycin resistance proteins VanH and VanA, *Biochemistry 30*, 10408−10415.

BI049496D